Received: 04 January 2025 | **Revised:** 16 May 2025 | **Accepted:** 22 May 2025 Science Research Annals—Physical Sciences 1(1), 10–23

SCIENCE RESEARCH ANNALS
(PHYSICAL SCIENCES)

Published by Faculty of Science, Adekunle Ajasin University, Akungba-Akoko (AAUA)

Journal website: https://sra.com.ng/index.php/sra-physical

SCIENTIFIC ARTICLE DOI: https://doi.org/10.63112/gs3g1g80

In Silico evaluation of the potential of phytochemicals from *Cissus populnea* against *Mycobacterium* tuberculosis

Oluwatoba Emmanuel Oyeneyin [1, *]

[1] *Theoretical and Computational Chemistry Unit, Department of Chemical Sciences, Adekunle Ajasin University, 001 Akungba-Akoko, Ondo State, Nigeria*

*Correspondence: oluwatoba.oyeneyin@aaua.edu.ng; emmanueltoba90@gmail.com (O.E. Oyeneyin)

ARTICLE INFORMATION

Keywords:
Cissus populnea
Phytochemicals
Mycobacterium tuberculosis
Molecular docking
Molecular dynamics simulation

Handling Editor: M.B. Aminu

Disclaimer: All opinions expressed are solely the authors, and do not necessarily represent that of the Journal's Editorial Board, Management, or workers.

ABSTRACT

The study investigated the anti-tubercular potential of the phytochemicals of the extracts of *Cissus populnea* (*C. populnea*) via *in silico* methods. Some phytochemicals from the plant were screened against *Mycobacterium tuberculosis* type II dehydroquinase (MTBII DHQase) and *Pantothenate Synthetase* (PS) using molecular docking techniques. Against MTBII DHQase, luteolin and catechin had the highest docking scores among the compounds from *C. populnea*, even higher than that of clofazimine, the reference drug. Against PS, the results also revealed that luteolin and poncirin had the highest scores among the compounds, also higher than that of pyrazinamide, a standard PS inhibitor. The compounds interacted with key amino acid residues in the proteins' binding pockets. Molecular dynamic simulation of the lead compounds revealed stability of the complexes at the binding pocket of the proteins, with the average root mean-squared deviation all below 2.5 Å. The best models generated from quantitative structure-activity relationships were kpls_desc_6 and kpls_desc_47, with standard deviation values of 0.405 and 0.7829, respectively, indicating closeness between the predicted and observed values, while the R^2 values were 0.7283 and 0.9156, respectively, underscoring the models' ability in making predictions. The model kpls_desc_6 predicted a pIC_{50} of 5.008 µM for catechin against MTBII DHQase, while the model kpls_desc_47 predicted pIC_{50}s of 5.407 µM and 5.362 µM for luteolin and poncirin, respectively, against PS. The fitness score generated by e-pharmacophore modeling showed that all compounds except cis-octadecanoic acid, methyl ester, scored above the standard drugs. Further clinical and preclinical investigations should be conducted on the phytochemicals from *C. populnea* in a bid to harness their full potential as anti-TB agents.

Highlights

- In this study, molecular docking was performed on some phytochemicals from *Cissus populnea* against *Mycobacterium tuberculosis* type II dehydroquinase (MTBII DHQase) and *Pantothenate Synthetase* (PS) in a bid to unravel their antitubercular potential.
- Reference drugs for the two targets (clofazimine and pyrazinamide for MTBII DHQase and PS, respectively) were also docked at the active sites of the proteins.
- The interactions of the phytochemicals and standard drugs with key amino acid residues of the proteins were identified.
- The stability of the complexes was revealed by the root-mean-squared deviation after molecular dynamics simulation for 100 ns.
- Luteolin and catechin had the best docking scores with MTBII DHQase, while luteolin and poncirin had the best docking scores with PS.

1. Introduction

Since ancient times, plants have always been used to boost the immune system and in the treatment and management of a lot of diseases. However, in recent times, about 80% of the world's population, most especially the developing and underdeveloped nations, rely mainly on natural products and plant metabolites for the treatment of several communicable and non-communicable diseases (Chin et al. 2006). This is not unconnected with the presence of secondary metabolites in these plants (Newman and Cragg 2012; Boucher et al. 2017). These secondary metabolites in plants have bioactive functional groups that offer a promising opportunity to hunt certain biological targets, which is a pivotal condition for drug discovery (Anand et al. 2019).

Tuberculosis (TB) is caused by *Mycobacterium tuberculosis* (MTB),

and it is very popular and regarded as one of the leading causes of death worldwide, with a lifetime risk of 5-10% (Ramaswamy and Musser 1998). This disease has infected about 2 billion people globally, and it causes about 4000 deaths per day and about 1.5 million deaths annually (Chai et al. 2020; Pai 2020). Also, there are an average of 15 million active tuberculosis cases yearly, with a substantial burden happening in India, Indonesia, Nigeria, South Africa, the Philippines, Bangladesh, Pakistan, and China (Bhargava and Bhargava 2020; Lv et al. 2024). According to the WHO, Nigeria had the highest TB cases in Africa and is ranked 6th among the countries with the highest cases of TB globally in 2018 (WHO, 2020). Nigeria's case is compounded by TB drug resistance and the prevalence of HIV/AIDS in the country (WHO, 2018). This is because people living with HIV/AIDS develop TB, with more than 63,000 cases of such reported (Ugwu et al. 2021), while 39,000 die from the disease each year (WHO, 2018). Reports indicate that Nigeria recorded about 80% of the global cases of TB in 2016 (Ugwu et al. 2021).

Although with the emergence of some anti-TB drugs such as isoniazid, ethambutol, rifampicin, and pyrazinamide in the mid-20th century, there was a sharp decline in the incidence of TB. However, in recent times, the trend has reversed as there was an increase in global TB cases owing to resistance issues (Hendrawati 2017). The misuse of anti-TB drugs, most especially in developing nations like Nigeria, resulted in the occurrence of this serious resistance. Globally, there were 175,650 multidrug resistant (MDR) and rifampicin resistant cases in 2022, even higher than what was reported in the previous year, 2021 (161,843 cases) and 2020 (150,510 cases) (WHO, 2023), with now over an estimated 360,000 - 440,000 cases reported in 2023 (WHO, 2024). The development of resistance by the microorganism, MTB, led to a decline in the efficacy of the first-line and second-line drugs in the treatment of TB. Also, second-line drugs such as ethionamide and capreomycin have been reported to have some disturbing safety issues while others, such as ofloxacin, with high efficacy, are too expensive for most countries to bear. Thus, the need to develop novel, efficacious, safer, and affordable anti-TB drugs with multi-domain inhibitory effects is of paramount importance.

Plants have an abundance of bioactive compounds and could play a pivotal role in curing diseases, and their resistant nature may be handled effectively. One such plant with numerous activities against various human diseases is *Cissus populnea* (*C. populnea*). It belongs to the family Vitaceae. *C. populnea* is widely distributed all over Nigeria, with local names such as "Okoho" in Idoma and Ighala people and "Ajara" or "*Orogbolo*" in Yoruba (Achikanu and Ani 2020). The extracts of different parts of this plant have been used for the treatment of sexual dysfunction, sore breasts, intestinal parasites, wounds, microbial infections, sickle cell, skin disease, and boils, among others (Aderolua et al. 2017; Nyemb et al. 2018; Uleh et al. 2018). It has also been reported for its glucose-reducing, antimalarial, antioxidant, and antimicrobial (Rotimi et al. 2023). Its extracts have also been reported to inhibit oxidative stress (Akomolafe et al. 2013). The antimicrobial activity of the plant has also been reported, albeit scantily. The only antimicrobial activity reported for the plant was against *S. aereus, E. coli, C. albicans,* and *T. mentagrophytes* (Alex-asaolu et al. 2024). These activities are due to the presence of various secondary metabolites such as vitamins, alkaloids, tannins, carotenoids, ascorbic acid, anthraquinones, saponins, phenolics, terpenoids, phytosterols, and so on (Rotimi et al. 2023). Surprisingly, its use as an anti-TB agent has hardly been reported. Also, there is a dearth of information on the identification of the actual compounds in the plant. One study that investigated the phytochemicals present in *C. populnea* was done in Nigeria by Mark and coworkers, where they identified the phytochemicals present in the stem of the plant in different locations in Benue State, Nigeria, using GC-MS (Uleh et al. 2018). They discovered that hexadecanoic acid (palmitic acid), methyl stearate, 6-octadecanoic acid were present in the ethyl acetate extracts of the plant in the different locations, while some compounds such as nonacos-1-ene, octadic-9-enoic acid, cis-octadecanoic acid, and so on, were present in some of the plant's stems picked from different locations. The variations in these chemicals in the different localities were attributed to different soil types. Most of these secondary metabolites are present in other plants and have also been reported for their anti-TB activities (Mishra et al. 2017; Tyagi et al. 2017). Specifically, hexadecanoic acid was reported to be present in the extract of leech and was active against MTB (Ojo et al. 2018). In the same vein, methyl stearate was reported to be an alternative as an anti-TB drug, a welcome development, especially as Bedaquiline and Delamanid have been reported for resistance against tuberculosis (Nirmal, C. R., Balasubramanian, M., Mohanvel et al. 2023). It is on this premise that we seek to investigate the compounds present in *C. populnea* for their anti-TB potential using *in silico* approaches such as molecular docking, molecular dynamic simulation, quantitative structure-activity relationship (QSAR), and pharmacophore modelling.

2. Methodology

2.1 Identification and collection of phytochemicals from Cissus polpunea

The phytochemicals from *C. populnea* were obtained from literature (Uleh et al. 2018; Ochekwu 2023) and downloaded from PubChem in their .sdf format. The compounds and their PubChem IDs are presented in Table 1.

2.1.1 Molecular docking

The compounds were imported into the Maestro/Schrodinger package (Schrödinger Release 2023-3: Maestro) and prepared using the LigPrep module (Schrödinger Release 2023-3: LigPrep) while the receptors (PDB IDs: 2Y71 and 1N2H) were downloaded from the Protein Data Bank (www.rcsb.org) and prepared using the protein preparation wizard (Madhavi Sastry et al. 2013) using the OPLS4 forcefield (Lu et al. 2021). The active sites of the receptors ($x = 7.26,\ y = -29.36,\ z = -47.45$ for $2Y71$; $x = 31.91,\ y = 34.28,\ z = 42.97$ for 1N2H) were determined using receptor grid generation module on the package. The ligands were docked at these active sites to obtain their binding affinities. The standard precision (SP) and the extra precision (XP) docking methods were employed for molecular docking.

2.1.2 Molecular dynamics simulation

The lead compounds, the standard drugs (clofazimine and pyrazinamide), and unbound proteins (APO) were solvated using the system builder on the Desmond module using the TIP3P water model (Florová et al. 2010) with the OPLS4 forcefield and 0.15 M sodium chloride salt. This solvent model has successfully been used in solvating complexes (Issahaku et al. 2023; Oyeneyin et al. 2024). The stability, flexibility, and protein-ligand contacts of the complexes were determined by molecular dynamics simulation, which was run for 100 ns using the NPT ensemble at 300 K and 10.013 bar pressure.

2.1.3 AutoQSAR model generation

Experimental data for inhibitors targeting 2Y71 and 1N2H were obtained from the CHEMBL database (www.ebi.ac.uk/chembl), including their corresponding pIC_{50} values. The dataset was converted to SDF format using DataWarrior (version 2) as described in (Omoboyowa 2022). These files were then imported into the Schrödinger workspace and prepared using the MacroModel tool. AutoQSAR models were generated based on the pIC_{50} values of the hit compounds, and the top-performing models were selected to predict the pIC_{50} values of the screened compounds. The models' parameters and plots with the predicted IC_{50} (pIC_{50}) are presented in the results section.

2.1.4 Generation of E-pharmacophore hypothesis and phase screening of compounds

The E-pharmacophore hypothesis was generated for the targets (2Y71 and 1N2H) with co-crystalized ligands through energy-optimized receptor-ligand pharmacophore of the Maestro suite. The compounds were prepared with macromodel minimization and screened by E-pharmacophore-based phase screening of the generated subset of the compounds that possess the requisite features for the target binding to the targets. The fitness scores of the compounds were estimated (Omoboyowa 2022) and interpreted in the results section.

3. Results and Discussion

3.1. Molecular docking

Molecular docking was performed at the defined active sites to assess binding affinities of the compounds against two anti-TB targets, namely, *Mycobacterium tuberculosis* type II dehydroquinase (MTBII DHQase) and *Pantothenate Synthetase* (PS). These targets are of interest in that MTBII DHQase, for instance, catalyzes the crucial dehydration step that converts 3-hydroquinate into 3-hydroshikimate in the shikimate pathway. This conversion helps the growth and survival of MTB. Therefore, inhibiting this process is crucial in blocking the MTB's growth (Nunes et al. 2020). Inhibitors of MTBII DHQase have been reported to show remarkable activity against *M. tuberculosis* (Gourley et al. 1994; Tran et al. 2012). PS is very crucial in the biosynthesis of Coenzyme A (which supports the bacteria's survival by aiding many metabolic processes) in MTB (Imran et al. 2024). It catalyzes the final step in the pantothenate biosynthesis in MTB, aiding its growth and severity (Ciulli et al. 2008). Targeting these enzymes is therefore necessary in a bid to arrive at more effective anti-TB drugs.

The docking results of the compounds are presented in Tables 1 and 2, respectively, against MTBII DHQase (PDB ID: 2Y71) and PS (PDB ID: 1N2H). Results revealed that luteolin (-8.543 kcal/mol and -9.005 kcal/mol, respectively, for SP and XP docking) and catechin (-7.718 kcal/mol and -8.006 kcal/mol, respectively, for SP and XP docking) had the highest binding affinities among the compounds from *C. populnea* against MTBII DHQase. Generally, cis-Octadecanoic aci-methyl ester, 2,4-Dimethylbenzo[h]quinoline, and poncirin, alongside the lead compounds (luteolin and catechin), had higher binding affinities than clofazimine (-5.478 kcal/mol and -4.268 kcal/mol, respectively, for SP and XP docking). Luteolin interacted with some residues of the protein, such as hydrogen bonding with ASN75 via its carbonyl oxygen, hydrogen bonding with HIS81 and ARG112 via its hydroxyl group, and pi-pi stacking interaction with TYR24 via its phenyl and chromenone rings (Figure 1). Catechin interacted and formed hydrogen bonds with ASN 12 via its hydroxyl group, ARG19 via hydrogen bonding with the hydroxyl group on its phenyl ring (Figure 2). Clofazimine formed halogen bonds with ASN75, HIP101, ILE102, and SER103 via its chlorine atom and pi-cation interaction with ARG15 via its phenyl ring (Figure 3). These inter-

Table 1: The phytochemicals in *Cissus populnea*, PubChem IDSs, docking scores/binding affinities against *Mycobacterium tuberculosis* type II dehydroquinase (PDB ID: 2Y71).

Compounds	PubChem ID	SP docking score (kcal/mol)	XP docking score (kcal/mol)
Hexadecanoic acid, methyl ester	8181	0.383	-0.331
Methyl stearate	8201	-0.280	0.436
6-Octadecanoic acid, (Z)-	16536780	-	-
Nonacos-1-ene	156989	-	-
Octadec-9-enoic acid	965	-1.042	-4.885
cis-Octadecanoic acid, methyl ester	91713067	-5.637	-6.660
Dodecanoic acid methyl ester	8139	0.494	-1.872
methyl tetradecanoate	31284	-0.181	0.108
Undecanoyl chloride	87287	-1.917	-3.839
9,12-Octadecanoic acid, methyl ester	5362793	-0.565	-0.575
9 -Octadecanoic acid (z)- methyl ester	5364509	-0.858	-0.445
2-Methyl –z,z-3,13-Octadecadienol	5364412	-1.579	-3.778
Heptadecanoic acid, 16-methyl, methyl ester	71587668	-2.537	-2.517
7- pentadecyne	117110	-0.630	-2.411
i-propyl 9-Octadecenoate	66981	-3.216	-4.727
Carbonic acid, But-3-en-1-yl, pentadecyl ester	91692457	-3.022	-2.953
2,4-Dimethylbenzo[h]quinoline	610182	-6.016	-4.432
n- Hexadecanoic acid	985	-0.607	-4.360
i-Propyl 9-tetradecenoate	56936038	-1.240	-3.208
poncirin	442456	-6.239	-7.385
nobiletin	72344	-5.957	-3.351
luteolin	5280445	-8.543	-9.005
catechin	73160	-7.718	-8.006
clofazimine	2794	-5.478	-4.268
Co-ligand	44468170	-8.886	-12.075

(−) *implies no docking scores*

actions, especially with the two most important residues in MTBII DHQase (ARG 19 and TYR 24), were reported in (Dias et al. 2011). Interactions with ARG 19, HIP101, and TYR 24 have been reported as crucial in the biology of MTBII DHQase (Liu et al. 2015). In their work, interactions with ASN 12, TYR 24, and ARG 19 were reported for the lead compound (AQ38-2) (Yapo et al. 2021). This is indicative that this plant could inhibit MTBII DHQase via the shikimate pathway.

Table 2: The phytochemicals in *Cissus populnea*, PubChem IDSs, docking scores/binding affinities against Pantothenate Synthetase (PDB ID: 1N2H).

Compounds	PubChem ID	SP docking score (kcal/mol)	XP docking score (kcal/mol)
Hexadecanoic acid, methyl ester	8181	-2.129	-5.775
Methyl stearate	8201	-1.580	-0.867
6-Octadecanoic acid, (Z)-	16536780	-	-
Nonacos-1-ene	156989	-	-
Octadec-9-enoic acid	965	-1.970	-0.876
cis-Octadecanoic acid, methyl ester	91713067	-6.462	-6.754
Dodecanoic acid methyl ester	8139	-0.124	-2.229
methyl tetradecanoate	31284	-0.290	-3.069
Undecanoyl chloride	87287	-	-
9,12-Octadecanoic acid, methyl ester	5362793	-1.417	-2.324
9 -Octadecanoic acid (z)- methyl ester	5364509	-1.101	-2.947
2-Methyl –z,z-3,13-Octadecadienol	5364412	-3.858	-2.715
Heptadecanoic acid, 16-methyl, methyl ester	71587668	-6.040	-
7- pentadecyne	117110	-0.989	-3.197
i-propyl 9-Octadecenoate	66981	-3.649	-4.127
Carbonic acid, But-3-en-1-yl, pentadecyl ester	91692457	-2.507	-4.314
2,4-Dimethylbenzo[h]quinoline	610182	-6.057	-4.299
n- Hexadecanoic acid	985	-1.314	-4.586
i-Propyl 9-tetradecenoate	56936038	-2.204	-3.953
poncirin	442456	-7.003	-6.457
nobiletin	72344	-4.691	-3.977
luteolin	5280445	-7.402	-8.120
catechin	73160	-6.366	-4.694
pyrazinamide	1046	-6.359	-5.110
Co-ligand	447261	-7.016	-8.234

(−) *implies no docking scores*

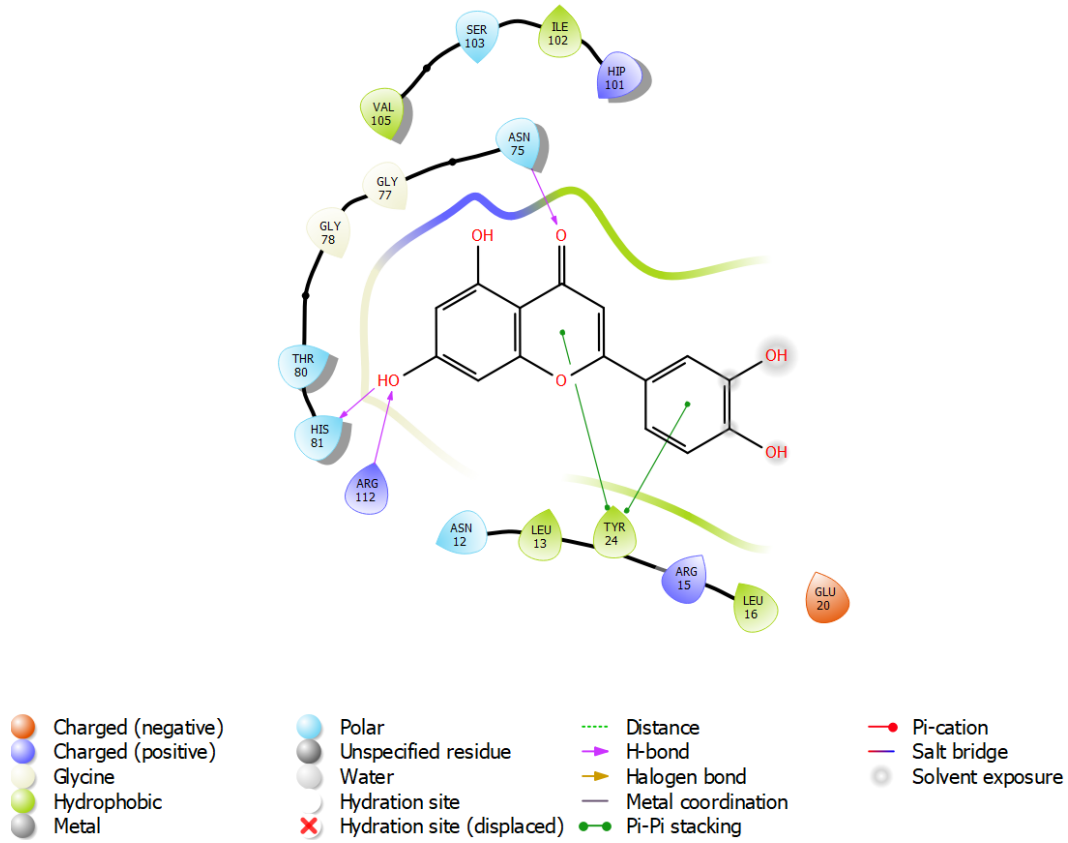

Figure 1: Bonding interactions between Luteolin and amino acid residues of 2Y71.

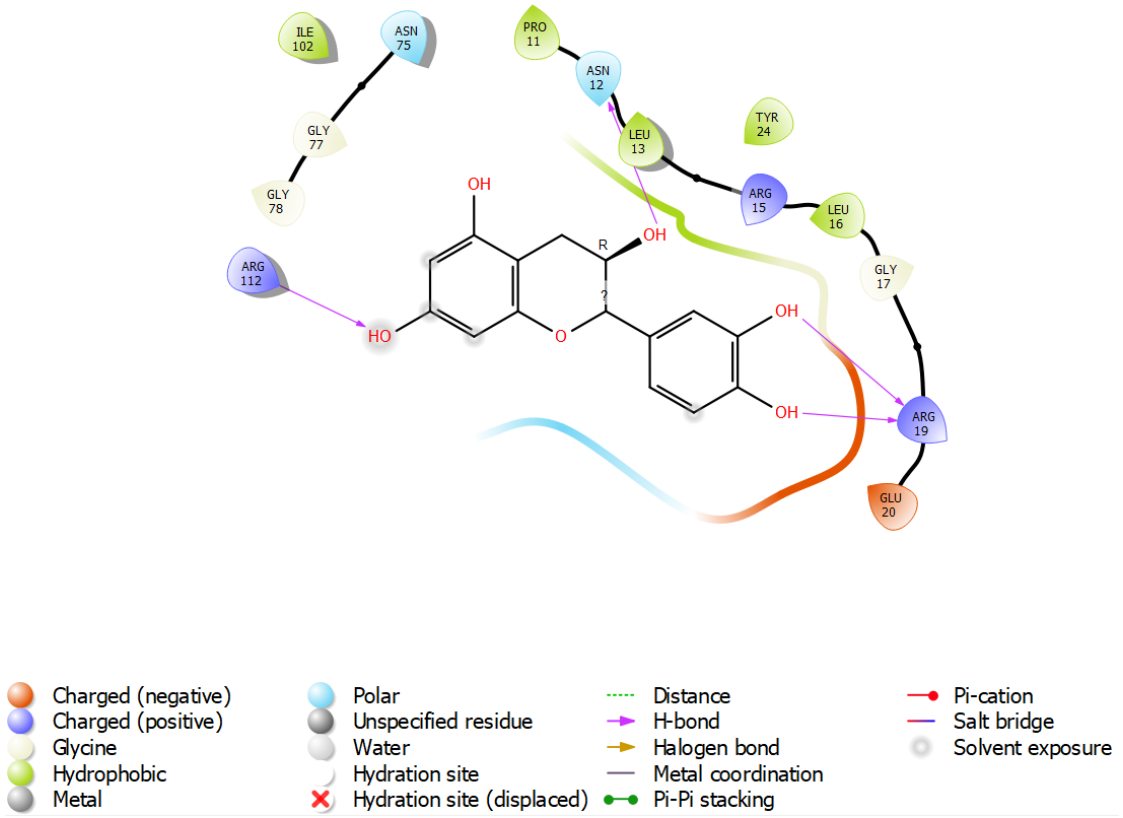

Figure 2: Bonding interactions between Catechin and amino acid residues of 2Y71.

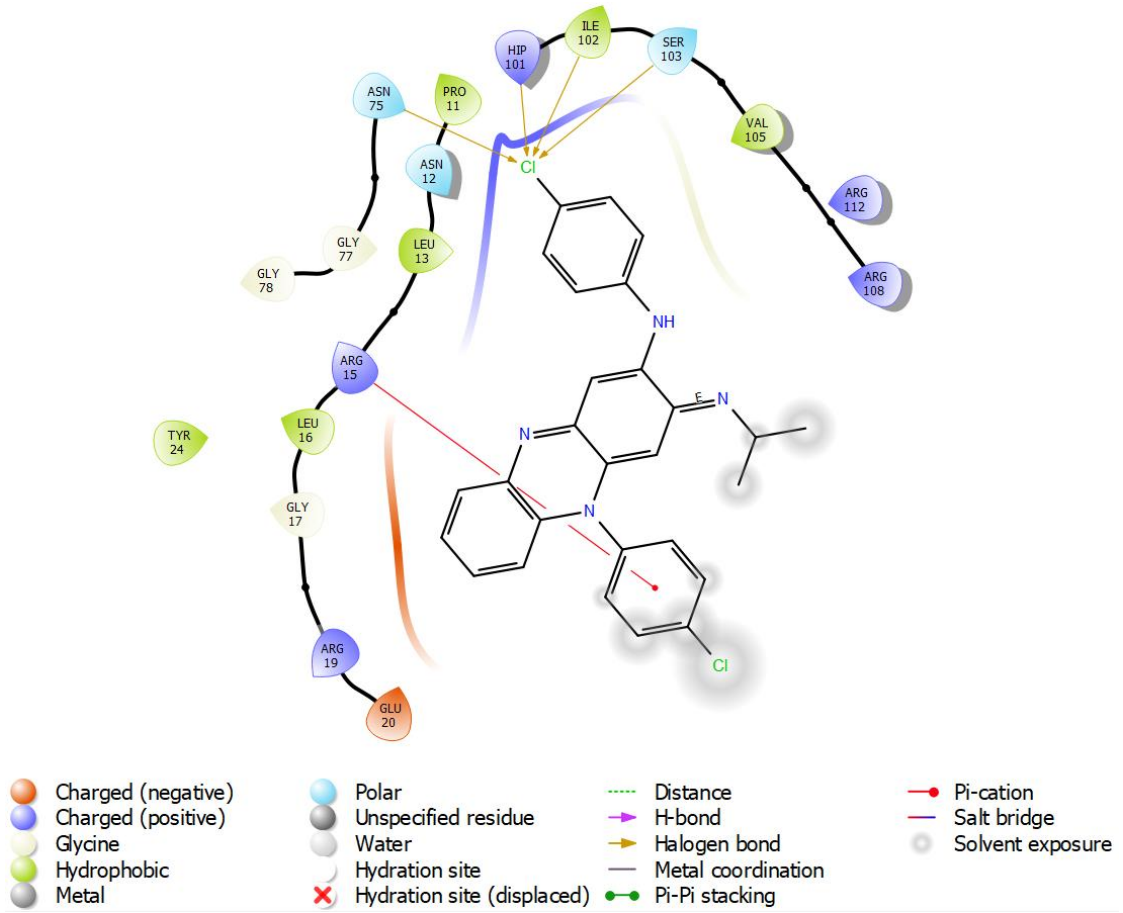

Figure 3: Bonding interactions between Clofazimine and amino acid residues of 2Y71.

Against PS, the results also revealed that poncirin and luteolin had the highest scores among the compounds from *C. populnea* while considering both SP and XP binding affinities. Both (poncirin, -7.003 kcal/mol and -6.457 kcal/mol for SP and XP docking, respectively) and (luteolin, -7.402 kcal/mol and -8.120 kcal/mol for SP and XP docking, respectively) had higher binding affinities with pyrazinamide (-6.359 kcal/mol and -5.110 kcal/mol for SP and XP docking, respectively). Poncirin interacted with PRO38, ASP161, and SER197, all hydrogen bonding via their hydroxyl groups (Figure 4). Luteolin displayed interactions with TYR82, SER197, SER196, MET195, VAL187, all hydrogen bonding via its hydroxyl groups, and with HIE44 (pi-pi stacking interaction via its chromenone ring (Figure 5). Pyrazinamide interacted with VAL187 via hydrogen bonding from its carbonyl and amine groups, MET195 via its amine group, and HIE44 due to pi-pi stacking with its pyrazine ring. (Figure 6). These interactions have been reported in several inhibitors of PS (Ntie-kang et al. 2014; Imran et al. 2024). In their work, all the amino acids interacting with the lead compounds and standard drug here were reported to be in the active site of PS (Chouhan et al. 2024); the compounds reported by them also interacted with most of these amino acids. This is an indication that *C. populnea* and its components can be explored as potential inhibitors of PS.

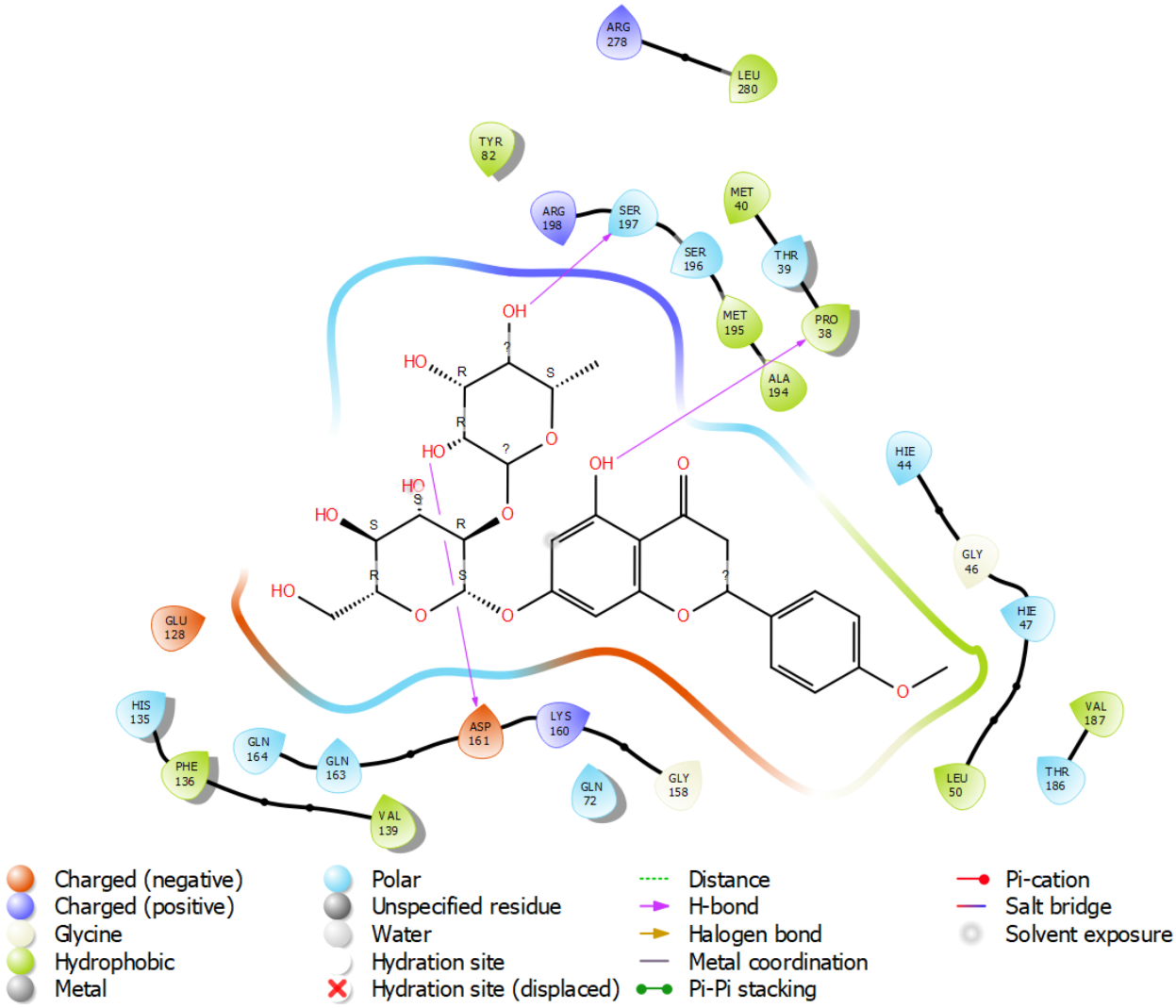

Figure 4: Bonding interactions between Poncirin and amino acid residues of 1N2H.

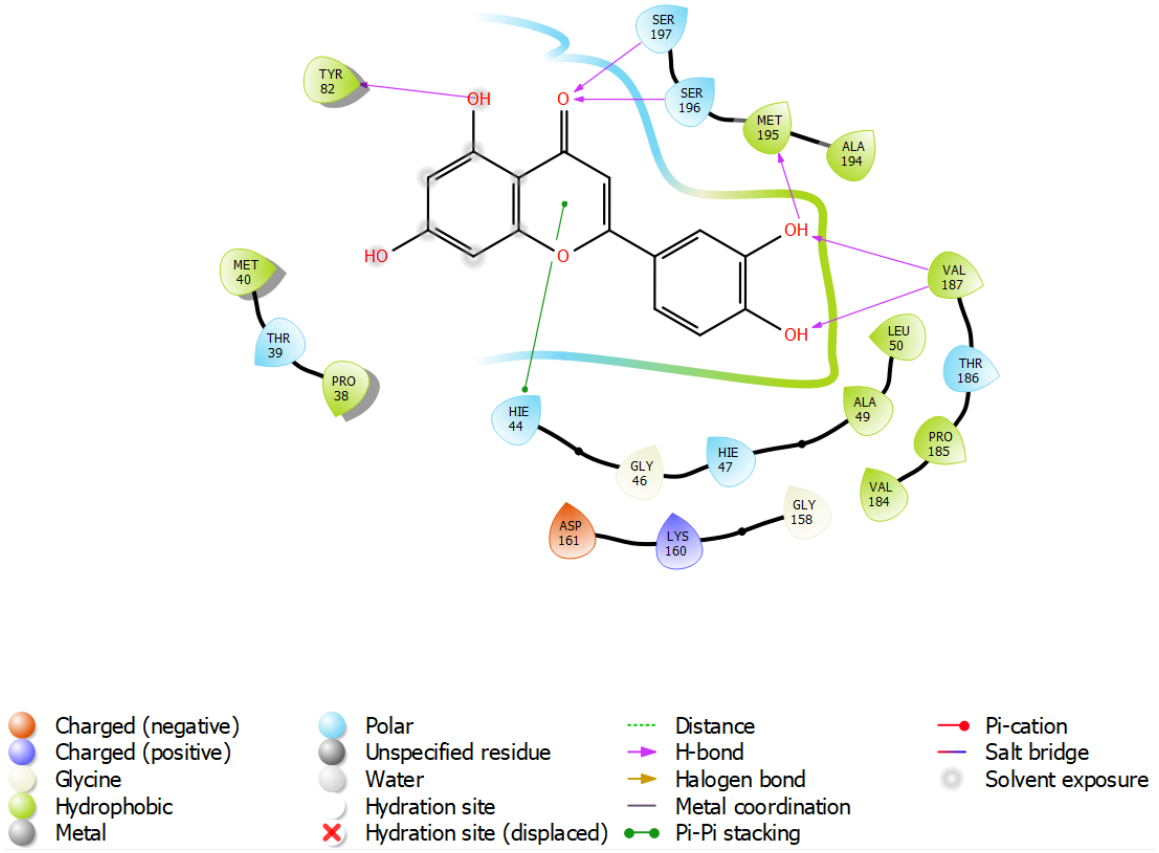

Figure 5: Bonding interactions between Luteolin and amino acid residues of 1N2H.

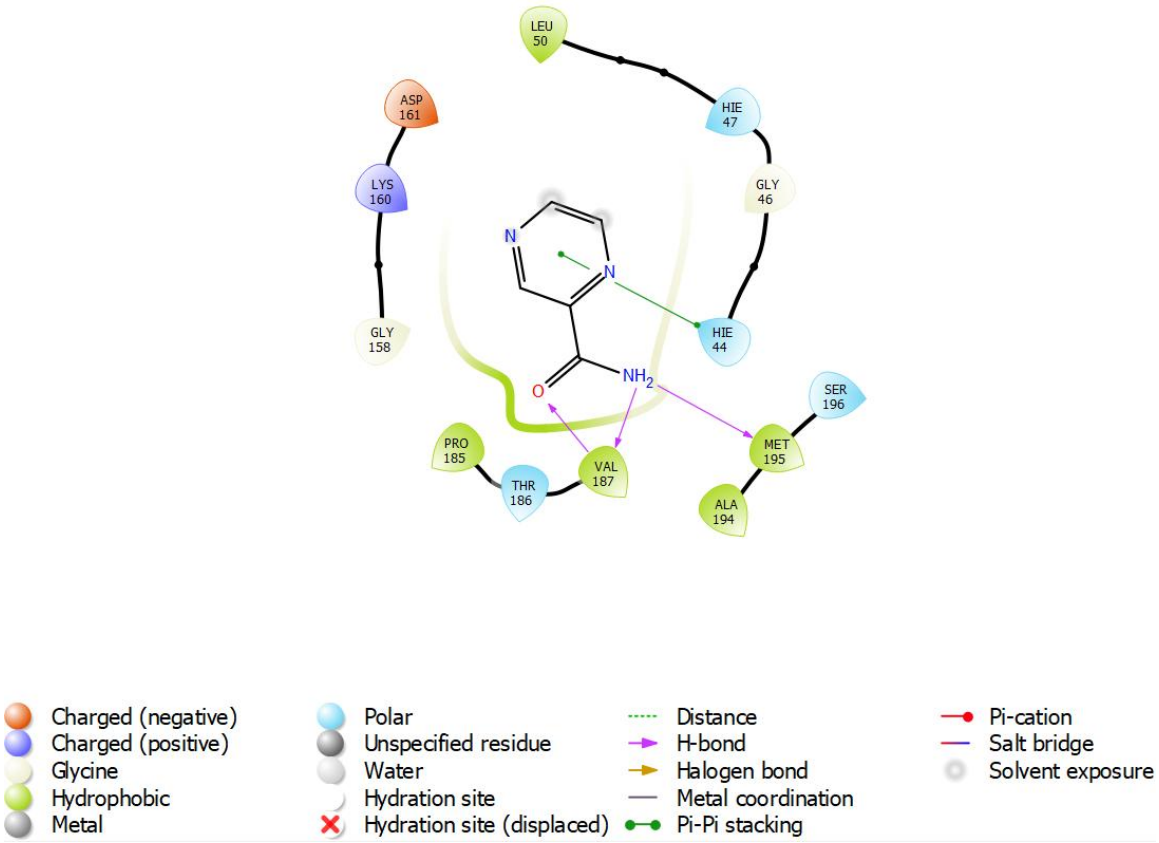

Figure 6: Bonding interactions between Pyrazinamide and amino acid residues of 1N2H.

3.2 MD results

The stability and flexibility of the complexes of the docked compounds and the proteins were determined by calculating the root mean squared deviation (RMSD) and fluctuation (RMSF) of the proteins' c-α. Their results (plots from the trajectories and averages and standard deviations) were compared with those of the unbound protein (APO) and presented in Figures 7–10 and Table 3. The average RMSD values of the complexes were lower than the unbound protein, indicating that the protein's c-α was more stabilized in the complexes (Table 3). The average RMSDs of the complexes were in the order APO (1.78±0.421) > Clofazimine (1.49±0.262) > catechin (1.44±0.227) > luteolin (1.42±0.191). The RMSD plot of the complexes (ligands-1N2H) is presented in Figure 8. The average RMSD values of the complexes were higher than the unbound protein, indicating that the protein's c-α were more stabilized in the APO state (Table 3). The average RMSDs of the complexes were in the order poncirin (2.13±0.307) > luteolin (2.11±0.352) > pyrazinamide (1.97±0.215) > APO (1.82±0.179). For both MTBII DHQase and PS, the average RMSD values suggest that the systems converged during the 100 ns since they remained below 2.5 Å, suggesting system convergence and stable simulations (Issahaku et al. 2022, 2023). The RMSD values indicated stability of the ligand-protein complexes.

The RMSF plots (Figures 9 and 10) showed that there were fluctuations in the residues of the proteins in the complexes. For MTBII DHQase, the compounds had higher potential to reduce the flexibility and increase the stability of the domain during binding, as seen from the average RMSF values in Table 3. The average RMSFs followed the order APO (0.927±0.575) > catechin (0.891±0.595) > clofazimine (0.886±0.517) > luteolin (0.706±0.356). Smaller RMSF values obtained for the ligand-protein complexes of MTB II DHQase in comparison to its APO state showed that the amino acid residues in the complexes were more rigid, hence minimal interactions with the ligands (Bhattacharya et al. 2024). For *Pantothenate Synthetase*, however, the average RMSFs followed the order poncirin (1.16±0.804) > luteolin (1.06±0.672) > pyrazinamide (1.01±0.553) > APO (0.894±0.429). This is indicative that the complexes have the tendency to possess more residual flexibility in the protein's c-α in PS, as it can be concluded from their average RMSD values as well, hence reduced stability as compared to the unbound protein.

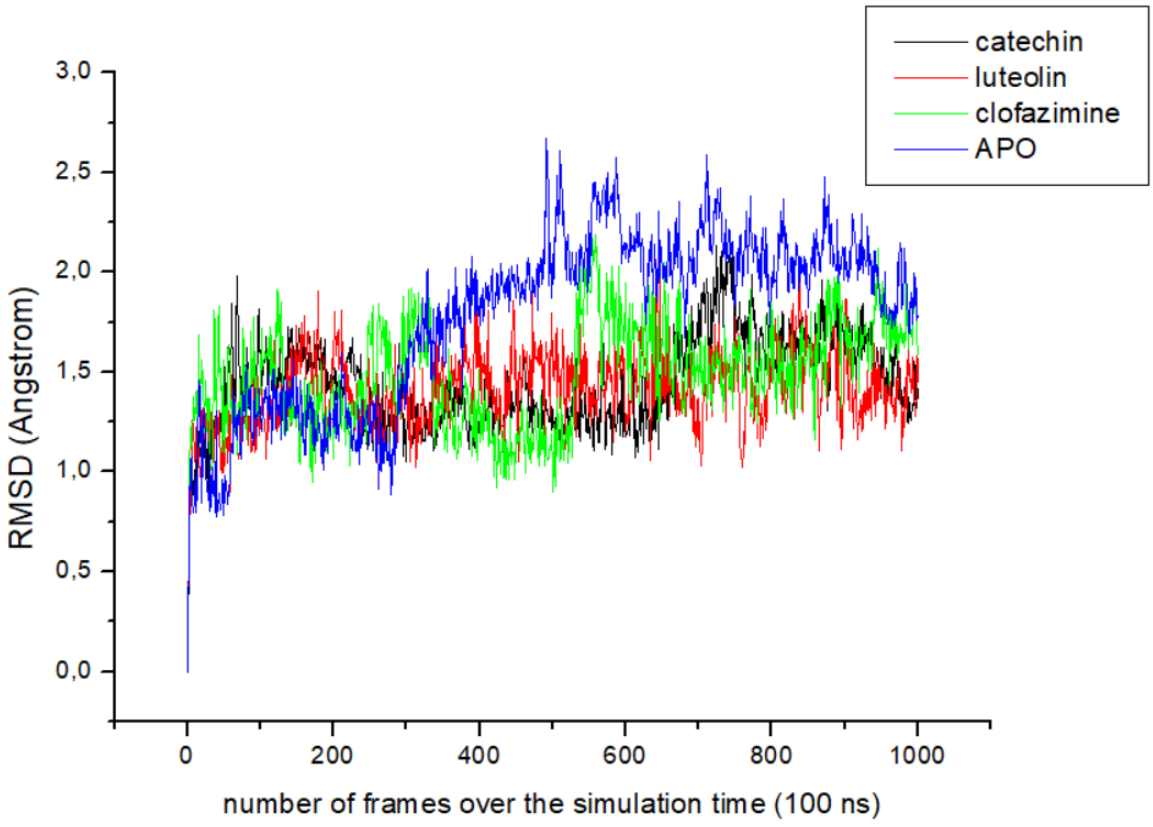

Figure 7: RMSD of the ligands-2Y71 complexes.

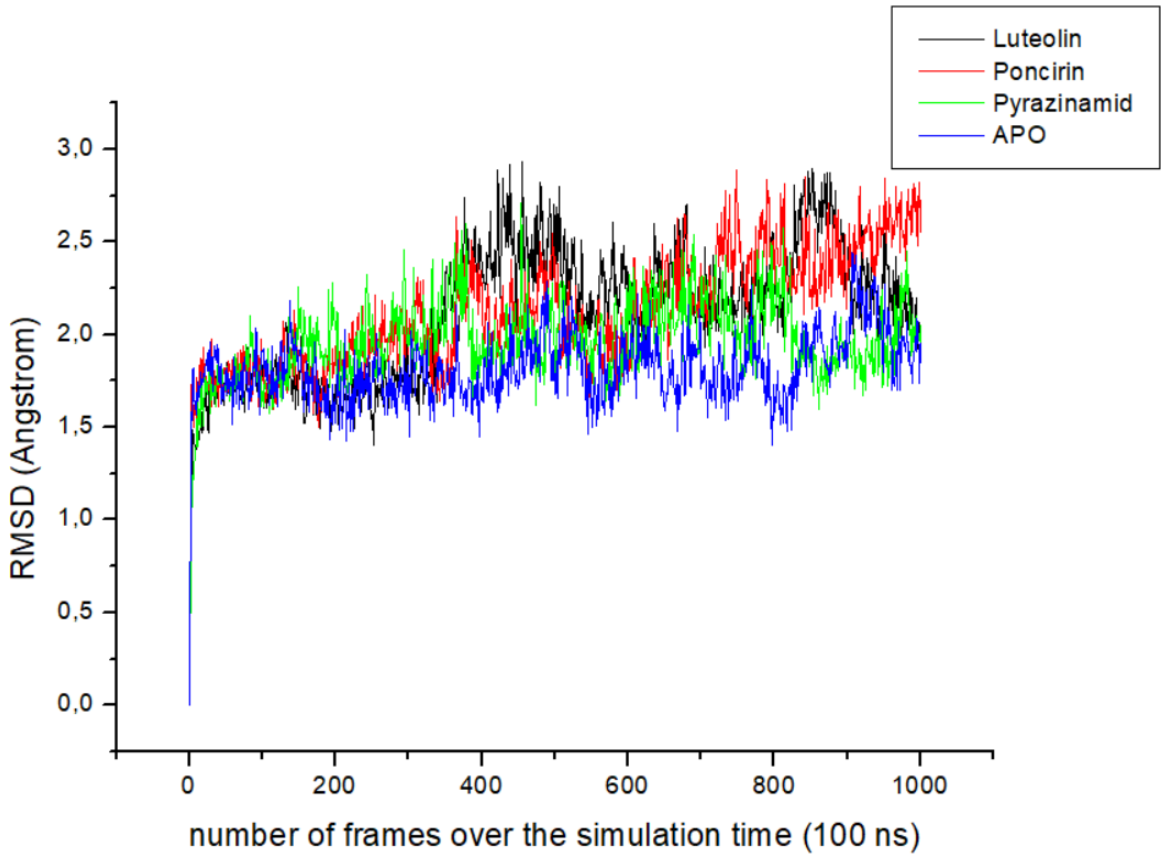

Figure 8: RMSD of the ligands-1N2H complexes.

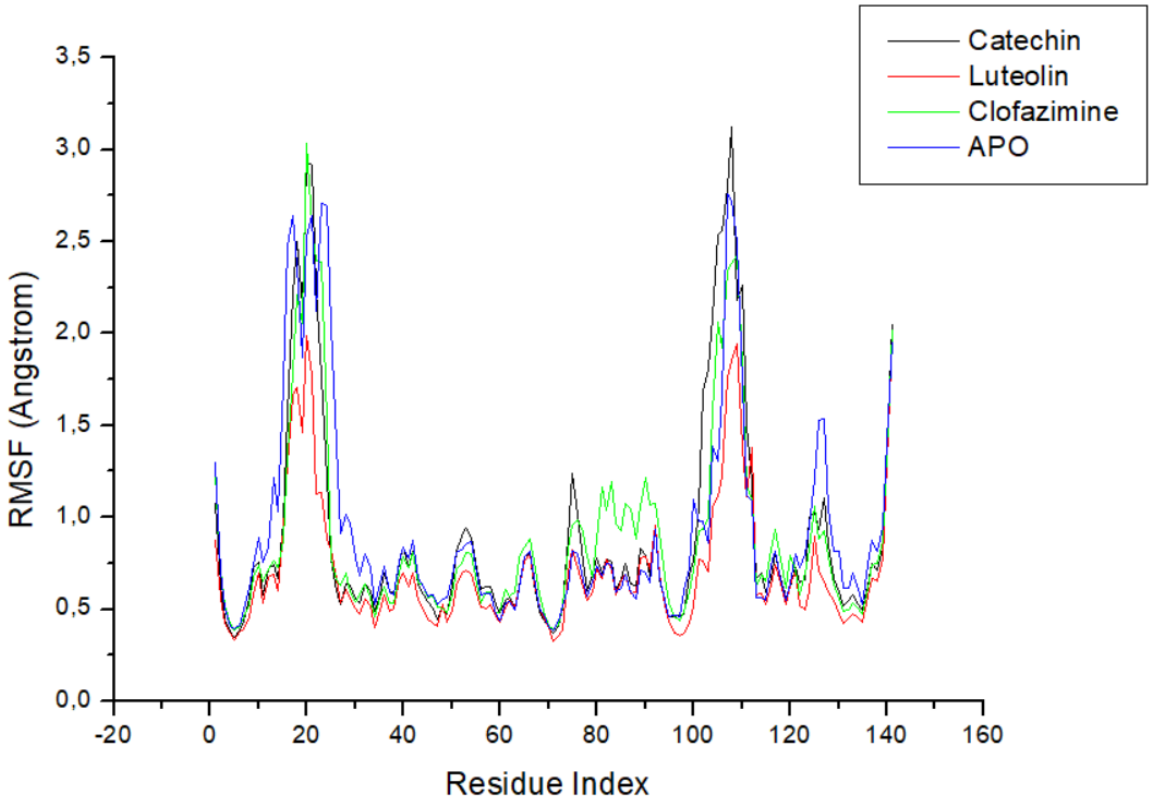

Figure 9: RMSF of the ligands-2Y71 complexes.

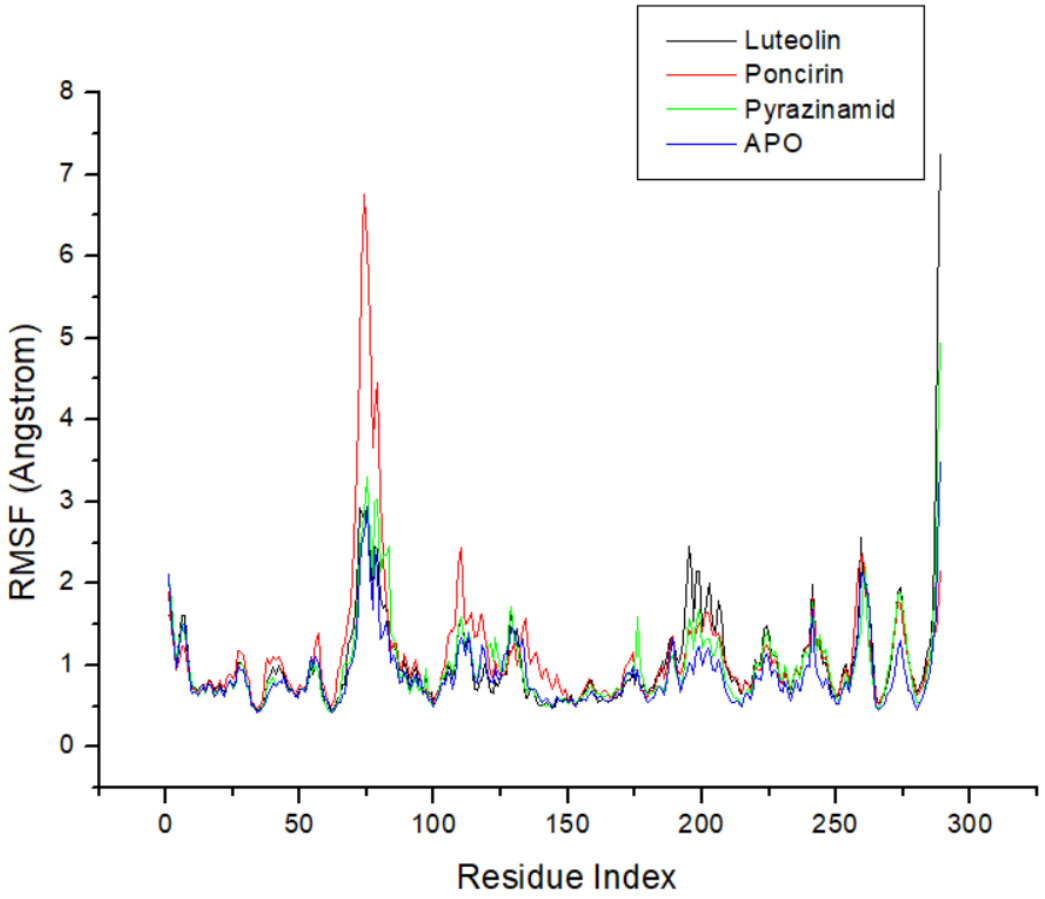

Figure 10: RMSF of the ligands-1N2H complexes.

Table 3: Average RMSD and RMSF values of the investigated complexes and their standard deviation (SD) values.

	RMSD (Å)		RMSF (Å)	
	Average	**SD**	**Average**	**SD**
2Y71-ligand complex				
Catechin	1.44	0.227	0.891	0.595
Luteolin	1.42	0.191	0.706	0.356
Clofazimine	1.49	0.262	0.886	0.517
APO	1.78	0.425	0.927	0.575
1N2H-ligand complex				
Luteolin	2.11	0.352	1.060	0.672
Poncirin	2.13	0.307	1.16	0.804
Pyrazinamide	1.97	0.215	1.01	0.553
APO	1.82	0.179	0.894	0.429

3.3 QSAR models

The model types for the two proteins are the non-linear multivariate regression model, the kernel partial least squares (KPLS) models. The best models for the two proteins were kpls_desc_6 and Kpls_desc_47 based on the ranking of all the models (Table 4). The precision of the models was analyzed using indices such as root-mean squared error (RMSE), standard deviation (SD), coefficient of determination (R^2), and cross-validation coefficient (Q^2) values. The RMSE values of these models were 0.8040 and 0.7063, respectively, for kpls_desc_6 and kpls_desc_47. This indicates that there are errors in the prediction, and the model fit is poor despite being the best among other models. The SD values of 0.4045 and 0.7829 for kpls_desc_6 and kpls_desc_47 respectively indicate that the predicted values are close to the observed values. R^2 values of 0.7283 and 0.9156 for kpls_desc_6 and kpls_desc_47, respectively, indicate a substantial ability of the model to make predictions. The predictive relevance of the model is established from the values of their Q^2, which were 0.6757 and 0.5602, respectively, for kpls_desc_6 and kpls_desc_47. The pIC_{50} values of the compounds and the reference drugs (Table 5) showed that the reference drugs have pIC_{50} values above 5.00 µM (5.265 µM and 6.359 µM) for clofazimine and pyrazinamide, respectively, while catechin proved to be the most satisfactory among the compounds against MTBII DHQase. For PS, luteolin and poncirin showed the most satisfactory pIC_{50}. The pharmacokinetics, drug-like properties, and toxicity of these compounds have been reported by previous researchers (Ahmed et al., 2022; Ali et

al., 2020; Chen et al., 2010; Luteolin et al., 2008; Ullah et al., 2022).

Table 4: AutoQSAR parameters of the best hypothesis.

Protein ID	Model code	RMSE	SD	R^2	Q^2
2Y71	kpls_desc_6	0.8040	0.4058	0.7283	0.6757
1N2H	Kpls_desc_47	0.7063	0.7829	0.9156	0.5602

Table 5: pIC_{50} predicted for the compounds according to the best model.

Pubchem ID	Compound Name	Predicted pIC_{50} (μM)	
		2Y71	1N2H
2794	Clofazimine (Ref. drug)	5.265	-
1046	Pyrazinamide (Ref. drug)	-	6.359
73160	Catechin	5.008	4.393
5280445	Luteolin	4.042	5.407
91713067	Cis-octadecanoic acid, methyl ester	3.371	4.473
442456	Poncirin	4.417	5.362

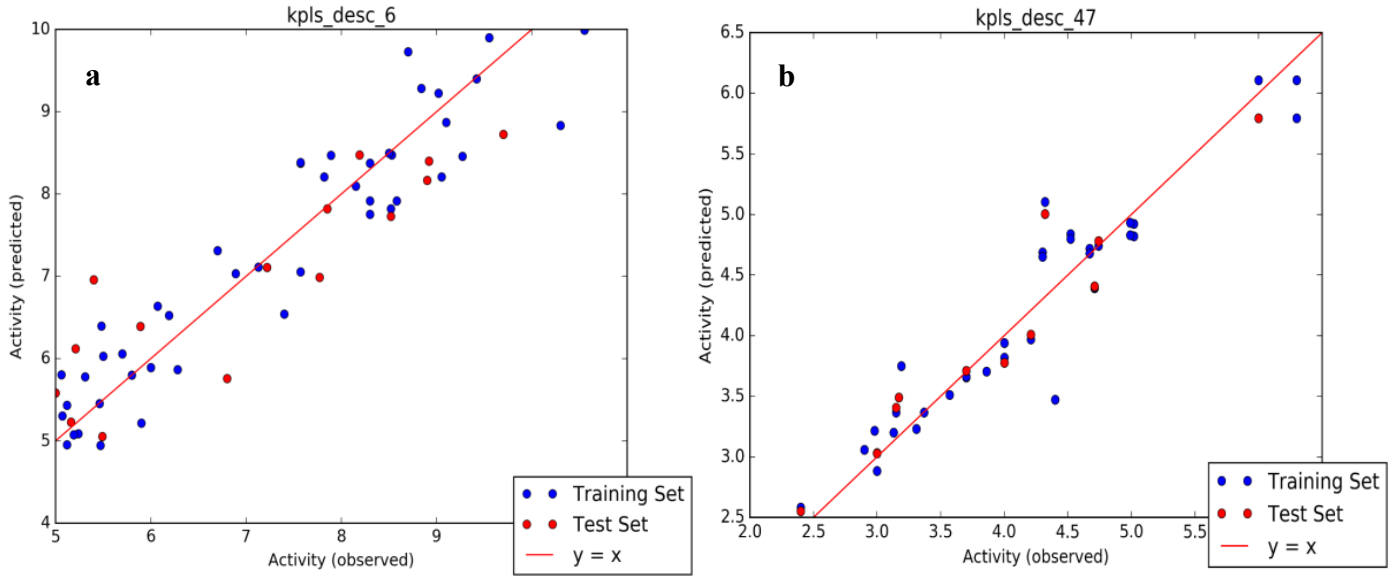

Figure 11: QSAR scatter plot (a) 2Y71 and (b) 1N2H.

3.4 E-pharmacophore hypothesis and fitness score evaluation

Auto-pharmacophore model from the lead compounds and their corresponding pIC_{50} was developed. In the pharmacophore hypothesis, the "fitness score" of a ligand refers to how well it aligns with the key features (pharmacophore) of a molecule known to interact with a target, like a protein. A higher score indicates a better fit and suggests a stronger potential binding interaction (Azam et al. 2020). Cis-octadecanoic acid, methyl ester showed a very poor fitness score, unlike others, catechin, luteolin, and poncirin scored above 1.0 with MTBII DHQase (Table 6). Catechin and luteolin also scored above 1.0 for PS, while poncirin scored below 1.0 (0.700). All compounds except cis-octadecanoic acid scored above the standard drugs.

Table 6: pIC_{50} predicted for the compounds according to the best model.

Pubchem ID	Compound Name	Fitness Score	
		2Y71	1N2H
2794	Clofazimine (Ref. drug)	0.213	-
1046	Pyrazinamide (Ref. drug)	-	0.692
73160	Catechin	1.843	1.027
5280445	Luteolin	1.945	1.446
91713067	Cis-octadecanoic acid, methyl ester	0.000	0.000
442456	Poncirin	1.334	0.7000

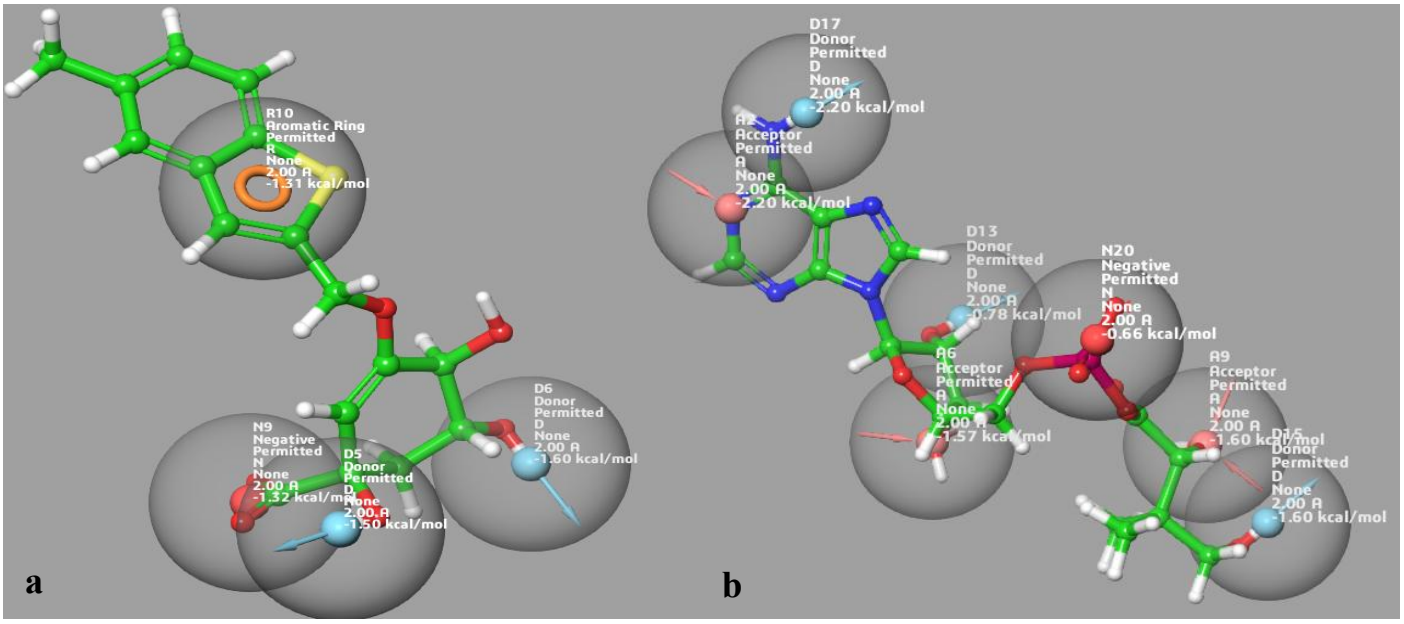

Figure 12: Hypothesis generated from targets-co-crystalized molecule complex (a) 2Y71 (b) 1N2H.

4. Conclusion

Natural compounds have been used as therapeutic agents for different kinds of diseases. In this work, some phytochemicals from *C. populnea* were docked at the defined active sites of two *Mycobacterium tuberculosis* targets (*Mycobacterium tuberculosis* type II dehydroquinase, MTBII DHQase, and *Pantothenate Synthetase*, PS) in a bid to assess their binding affinities. Further studies include molecular dynamics simulation to unravel the stability and/or flexibility of the docked complexes, quantitative structure-activity relationship to predict the bioactivity, and pharmacophore modelling to unravel the fitness scores of the models used. Molecular docking study revealed that luteolin (-8.543 kcal/mol and -9.005 kcal/mol for SP and XP docking respectively) and catechin (-7.718 kcal/mol and -8.006 kcal/mol for SP and XP docking respectively) had higher scores than clofazimine (-5.478 kcal/mol and -4.268 kcal/mol for SP and XP docking respectively). For PS, poncirin (-7.003 kcal/mol and -6.457 kcal/mol for SP and XP docking respectively) and luteolin (-7.402 kcal/mol and -8.120 kcal/mol for SP and XP docking respectively) had higher scores than pyrazinamide (-6.359 kcal/mol and -5.110 kcal/mol for SP and XP docking respectively). The interactions shown by the compounds and amino acid residues in the proteins are similar to those reported for inhibitors of MTBII DHQase and PS. Molecular dynamics simulation established the stability and flexibility of the complexes. For both targets, the average RMSD values suggest convergence of the systems as they were all below 2.5 Å, underscoring the confidence of the simulation process. The best models generated from quantitative structure-activity relationships gave standard deviation values of 0.405 and 0.7829, indicating that the predicted and observed values are close. R^2 values of 0.7283 and 0.9156, underscoring the models' ability to make predictions. The models predicted a pIC_{50} of 5.008 µM for catechin against MTBII DHQase and 5.407 µM and 5.362 µM for luteolin and poncirin, respectively, against PS. The fitness score generated by e-pharmacophore modeling showed that all compounds except cis-octadecanoic acid, methyl ester, scored above the standard drugs. The limitation of this study, however, is that only preliminary investigations are reported here, via *in silico* methods. It is recommended that the phytochemicals from *C. populnea* should be investigated further in a bid to harness their full potential as anti-TB agents via *in vivo* and *in vitro* investigations.

Acknowledgments

The author acknowledges Adekunle Ajasin University for creating an enabling environment to carry out this research work. All computational calculations were carried out using resources at the Centre for High-Performance Computing (CHPC), Cape Town, South Africa.

Funding

Tertiary Education Trust Fund (TETFUND), from the Government of the Republic of Nigeria, for Postdoctoral Fellowship Award (TETF/ES/UNIV/ONDO STATE/TSAS/2021).

Competing Interest

This paper has not been published elsewhere in whole or in part. Furthermore, the author declares no conflicting interests in this manuscript.

Data Availability Statement

Data associated with this study are available on request from the corresponding author.

Ethics Approval

Not applicable.

References

Achikanu CE, Ani ON (2020) Nutritional and Phytochemical Content of Cissus populnea (Okoho) Stem Bark. Asian J Res Biochem 7:8–15. https://doi.org/10.9734/ajrb/2020/v7i330139

Aderolua AZ, Lawal MO, Okoronkwo LI, et al (2017) Dietary effect of Cissus

populnea and Securidaca longepedunculata aqueous leave extracts on reproductive, haematological and biochemical parameters of African catfish Clarias gariepinus (Burchell, 1822) broodstocks. Aceh J Anim Sci 2:1–11. https://doi.org/10.13170/ajas.2.1.6138

Ahmed SA, Salau S, Khan A, Saeed M (2022) Inhibitive Property of Catechin and Chlorogenic Acid against Human Pancreatic Lipase: Molecular Docking and Molecular Dynamics Simulation Investigations. Adv J Chem A 5:226–240

Akomolafe SF, Oboh G, Akindahunsi AA, et al (2013) Inhibitory Effect of Aqueous Extract of Stem Bark of Cissus populnea on Ferrous Sulphate- and Sodium Nitroprusside-Induced Oxidative Stress in Rat's Testes In Vitro. ISRN Pharmacol 2013:1–7. https://doi.org/10.1155/2013/130989

Alex-asaolu A, Uba A, Birnin-yauri UA, Yusuf AJ (2024) Isolation and Characterization of Antimicrobial Constituent(s) from the Stem of Cissus populnea Guill. & Perr. drugs. drug candidates 3:172–183

Ali Y, Zaib S, Rahman MM, et al (2020) Poncirin, an orally active flavonoid exerts antidiabetic complications and improves glucose uptake activating PI3K/Akt signaling pathway in insulin resistant C2C12 cells with anti-glycation capacities Poncirin, an orally active flavonoid exerts antidiabet. Bioorg Chem 102:104061. https://doi.org/10.1016/j.bioorg.2020.104061

Anand U, Jacobo-Herrera N, Altemimi A, Lakhssassi N (2019) A comprehensive review on medicinal plants as antimicrobial therapeutics: Potential avenues of biocompatible drug discovery. Metabolites 9:1–13. https://doi.org/10.3390/metabo9110258

Azam MA, Thathan J, Jupudi S (2020) Pharmacophore modeling, atom based 3D-QSAR, molecular docking and molecular dynamics studies on Escherichia coli ParE inhibitors. Comput Biol Chem 84:107197. https://doi.org/10.1016/j.compbiolchem.2019.107197

Bhargava A, Bhargava M (2020) Tuberculosis deaths are predictable and preventable: Comprehensive assessment and clinical care is the key. J Clin Tuberc Other Mycobact Dis 19:100155. https://doi.org/10.1016/j.jctube.2020.100155

Bhattacharya S, Khanra PK, Dutta A, et al (2024) Computational Screening of T-Muurolol for an Alternative Antibacterial Solution against Staphylococcus aureus Infections: An In Silico Approach for Phytochemical-Based Drug Discovery. Int J Mol Sci 25:

Boucher HW, Ambrose PG, Chambers HF, et al (2017) White paper: Developing antimicrobial drugs for resistant pathogens, narrow-spectrum indications, and unmet needs. J Infect Dis 216:228–236. https://doi.org/10.1093/infdis/jix211

Chai Q, Wang L, Liu CH, Ge B (2020) New insights into the evasion of host innate immunity by Mycobacterium tuberculosis. Cell Mol Immunol 17:901–913. https://doi.org/10.1038/s41423-020-0502-z

Chen X, Liu L, Sun Z, et al (2010) Pharmacokinetics of luteolin and tetra-acetyl-luteolin assayed by HPLC in rats after oral administration. Biomed Chromatogr 826–832. https://doi.org/10.1002/bmc.1370

Chin Y-W, Balunas MJ, Chai HB, Kinghorn AD (2006) Drug discovery from natural sources. AAPS J 8:E239–E253. https://doi.org/10.1007/bf02854894

Chouhan M, Tiwari PK, Mishra R, et al (2024) Unearthing phytochemicals as natural inhibitors for pantothenate synthetase in Mycobacterium tuberculosis: A computational approach. Front Pharmacol 15:1–19. https://doi.org/10.3389/fphar.2024.1403900

Ciulli A, Scott DE, Ando M, et al (2008) Inhibition of Mycobacterium tuberculosis Pantothenate Synthetase by Analogues of the Reaction Intermediate. ChemBioChem 9:2606–2611. https://doi.org/10.1002/cbic.200800437

Dias MVB, Snee W, Bromfield KM, et al (2011) Structural investigation of inhibitor designs targeting 3-dehydroquinate dehydratase from the shikimate pathway of Mycobacterium tuberculosis. Biochem J 436:729–739

Florová P, Sklenovský P, Banáš P, Otyepka M (2010) Explicit water models affect the specific solvation and dynamics of unfolded peptides while the conformational behavior and flexibility of folded peptides remain intact. J Chem Theory Comput 6:3569–3579. https://doi.org/10.1021/ct1003687

Gourley DG, Coggins JR, Isaacs NW, et al (1994) Crystallization of a type II dehydroquinase from Mycobacterium tuberculosis. J Mol Biol 241:488–491. https://doi.org/10.1006/jmbi.1994.1524

Hendrawati (2017) An overview of phytotherapeutic approaches for the treatment of tuberculosis. Mini Rev Med Chem 17:167–183

Imran M, Abida, Guetat A, et al (2024) An Extensive Computational Investigation of Mycobacterium tuberculosis Pantothenate Synthetase Inhibitors from Diverse-Lib Compounds Library. ChemistrySelect 9:. https://doi.org/10.1002/slct.202402091

Issahaku AR, Aljoundi A, Soliman MES (2022) Establishing the mutational effect on the binding susceptibility of AMG510 to KRAS switch II binding pocket: Computational insights. Informatics Med Unlocked 30:100952. https://doi.org/10.1016/j.imu.2022.100952

Issahaku AR, Ibrahim MAA, Mukelabai N, Soliman MES (2023) Intermolecular And Dynamic Investigation of The Mechanism of Action of Reldesemtiv on Fast Skeletal Muscle Troponin Complex Toward the Treatment of Impaired Muscle Function. Protein J 42:263–275. https://doi.org/10.1007/s10930-023-10091-y

Liu C, Liu Y, Sun Q, et al (2015) Unraveling the kinetic diversity of microbial 3-dehydroquinate dehydratases of shikimate pathway. AMB Express 5:1–9. https://doi.org/10.1186/s13568-014-0087-y

Lu C, Wu C, Ghoreishi D, et al (2021) OPLS4: Improving force field accuracy on challenging regimes of chemical space. J Chem Theory Comput 17:4291–4300. https://doi.org/10.1021/acs.jctc.1c00302

Luteolin P, Rats M, Sarawek S, et al (2008) Pharmacokinetics of Luteolin and Metabolites in Rats. Nat Prod Commun 3:2029–2036

Lv H, Wang L, Zhang X, et al (2024) Further analysis of tuberculosis in eight high-burden countries based on the Global Burden of Disease Study 2021 data. Infect Dis poverty 13:70. https://doi.org/10.1186/s40249-024-01247-8

Madhavi Sastry G, Adzhigirey M, Day T, et al (2013) Protein and ligand preparation: Parameters, protocols, and influence on virtual screening enrichments. J Comput Aided Mol Des 27:221–234. https://doi.org/10.1007/s10822-013-9644-8

Mishra SK, Tripathi G, Kishore N, et al (2017) Drug development against tuberculosis: Impact of alkaloids. Eur J Med Chem 137:504–544. https://doi.org/10.1016/j.ejmech.2017.06.005

Newman DJ, Cragg GM (2012) Natural products as sources of new drugs over the 30 years from 1981 to 2010. J Nat Prod 75:311–335. https://doi.org/10.1021/np200906s

Nirmal, C. R., Balasubramanian, M., Mohanvel SK, Aathi MS, Munishankar S, et al (2023) Myoinositol and methyl stearate increases rifampicin susceptibility among drug-resistant Mycobacterium tuberculosis expressing Rv1819c. Chem Biol Drug Des 101:883–895

Ntie-kang F, Kannan S, Wichapong K, et al (2014) Binding of pyrazole-based inhibitors to Mycobacterium tuberculosis pantothenate synthetase: docking and MM-GB(PB)SA analysis†. Mol Biosyst 10:1–18. https://doi.org/10.1039/c3mb70449a

Nunes JES, Duque MA, Freitas TF De, et al (2020) Mycobacterium tuberculosis Shikimate Pathway Enzymes as Targets for the Rational Design of Anti-Tuberculosis Drugs. Molecules 25:

Nyemb J, Ndoubalem R, Talla E, et al (2018) DPPH antiradical scavenging, anthelmintic and phytochemical studies of Cissus poulnea rhizomes. Asian Pac J Trop Med 11:280–284. https://doi.org/10.4103/1995-7645.231468

Ochekwu E (2023) Nutraceutical Potentials of Cissus Populnea Linn Cultivated in the Southern Guinea Savanna Agroecology of Nigeria. Glob J Sci Front Res C Biol Sci 22:

Ojo PO, Babayi H, Olayemi IK, et al (2018) Anti-Tubercular Activities and Molecular Characterization of Salivary Extract of Leech [Hirudo medicinalis] against Mycobacterium tuberculosis. J Tuberc Res 06:1–9. https://doi.org/10.4236/jtr.2018.61001

Omoboyowa DA (2022) Exploring molecular docking with E-pharmacophore and QSAR models to predict potent inhibitors of 14-α-demethylase protease from Moringa spp. Pharmacol Res - Mod Chinese Med 4:100147. https://doi.org/10.1016/j.prmcm.2022.100147

Oyeneyin OE, Moodley R, Mashaba C, et al (2024) In vitro antiplasmodium and antitrypanosomal activities, β-haematin formation inhibition, molecular docking and DFT computational studies of quinoline-urea-benzothiazole hybrids. Heliyon 10:e38434. https://doi.org/10.1016/j.heliyon.2024.e38434

Pai M (2020) Tuberculosis: the story after the Primer. Nat Rev Dis Prim 6:. https://doi.org/10.1038/s41572-020-0161-5

Ramaswamy S, Musser JM (1998) Molecular genetic basis of antimicrobial agent resistance in Mycobacterium tuberculosis: 1998 update. Tuber Lung Dis 79:3–29. https://doi.org/10.1054/tuld.1998.0002

Rotimi DE, Evbuomwan IO, Iyobhebhe ME, et al (2023) Pharmacological activities of Cissus populnea in human diseases. Biocatal Agric Biotechnol 50:102719

Schrödinger Release 2023-3: Maestro, Schrödinger

Schrödinger Release 2023-3: LigPrep, Schrödinger, LLC, New York, NY, 2023

Tran AT, West NP, Britton WJ, Payne RJ (2012) Elucidation of Mycobacterium tuberculosis Type II Dehydroquinase Inhibitors using a Fragment Elaboration Strategy. ChemMedChem 7:1031–1043. https://doi.org/10.1002/cmdc.201100606

Tyagi G, Singh P, Varma-Basil M, Bose M (2017) Role of Vitamins B, C, and D in the Fight against Tuberculosis. Int J Mycobacteriology 6:239–245. https://doi.org/10.4103/ijmy.ijmy

Ugwu KO, Agbo MC, Ezeonu IM (2021) Prevalence of tuberculosis, drug-resistant tuberculosis and hiv/tb co-infection in Enugu, Nigeria. Heart Int 15:24–30. https://doi.org/10.21010/ajidv15i2.5

Uleh M, Vershima A, Ojogbayi S (2018) Phytochemical studies of Cissus populnea in Benue State, Nigeria. GSC Biol Pharm Sci 2:009–015.

https://doi.org/10.30574/gscbps.2018.2.1.0022
Ullah H, Khan A, Bibi T, et al (2022) Comprehensive in vivo and in silico approaches to explore the hepatoprotective activity of poncirin against paracetamol toxicity. Naunyn Schmiedebergs Arch Pharmacol 195–215. https://doi.org/10.1007/s00210-021-02192-1
WHO (2023). https://www.who.int/teams/global-tuberculosis-programme/tb-reports/global-tuberculosis-report-2023/tb-diagnosis---treatment/drug-resistant-tb-treatment. 2023
WHO (2024). https://www.who.int/teams/global-programme-on-tuberculosis-and-lung-health/tb-reports/global-tuberculosis-report-2024/tb-disease-burden/1-3-drug-resistant-tb. 2024
Yapo YM, Bosson J, Dali B, et al (2021) Computer-Aided Virtual Design of 3-Dehydroquinic Acid Analogues Inhibitors of Dehydroquinase Type II of Mycobacterium tuberculosis with Favorable Pharmacokinetics Profile. J Comput Chem Mol Model 5:640–656. https://doi.org/10.25177/JCCMM.5.3.RA.10774

How to Cite: Oyeneyin, O.E. (2025). *In Silico* evaluation of the potential of phytochemicals from *Cissus populnea* against *Mycobacterium tuberculosis*. *Science Research Annals–Physical Sciences,* 1(1), 10–23. https://doi.org/10.63112/gs3g1g80